

This discussion paper is/has been under review for the journal Hydrology and Earth System Sciences (HESS). Please refer to the corresponding final paper in HESS if available.

Transboundary geophysical mapping of geological elements and salinity distribution critical for the assessment of future sea water intrusion in response to sea level rise

F. Jørgensen¹, W. Scheer², S. Thomsen³, T. O. Sonnenborg⁴, K. Hinsby⁴,
H. Wiederhold⁵, C. Schamper⁶, T. Burschil⁵, B. Roth⁶, R. Kirsch², and E. Auken⁶

¹Geological Survey of Denmark and Greenland, Lyseng Allé 1, 8270 Højbjerg, Denmark

²State Agency for Agriculture, Environment and Rural Areas of the Federal State Schleswig-Holstein, Hamburger Chaussee 25, 24220 Flintbek, Germany

³Danish Nature Agency Ribe, Sorsigvej 35, 6760 Ribe, Denmark

⁴Geological Survey of Denmark and Greenland, Øster Voldgade 10, 1350 København K, Denmark

Transboundary geophysical mapping of geological elements

F. Jørgensen et al.

Title Page

Abstract

Introduction

Conclusions

References

Tables

Figures

⏪

⏩

◀

▶

Back

Close

Full Screen / Esc

Printer-friendly Version

Interactive Discussion

⁵Leibniz Institute for Applied Geophysics, Stilleweg 2, 30655 Hannover, Germany

⁶Dept. of Earth Sciences, Aarhus University, Høegh-Guldbergs Gade 2, 8000 Aarhus, Denmark

Received: 21 February 2012 – Accepted: 21 February 2012 – Published: 1 March 2012

Correspondence to: F. Jørgensen (flj@geus.dk)

Published by Copernicus Publications on behalf of the European Geosciences Union.

HESSD

9, 2629–2674, 2012

**Transboundary
geophysical mapping
of geological
elements**

F. Jørgensen et al.

Title Page

Abstract

Introduction

Conclusions

References

Tables

Figures



Back

Close

Full Screen / Esc

Printer-friendly Version

Interactive Discussion



Abstract

Geophysical techniques are increasingly used as tools for characterising the subsurface and they are generally required to develop subsurface models that properly delineate the distribution of aquifers and aquitards, salt/freshwater interfaces and geological structures that affect groundwater flow. In a study area covering 730 km² across the border between Germany and Denmark a combination of an airborne transient electromagnetic survey (performed with the SkyTEM system), a high-resolution seismic survey and borehole logging has been used in an integrated mapping of important geological, physical and chemical features of the subsurface. The spacing between flight lines is 200–250 m giving a total of about 3200 line km. About 38 km of seismic lines have been collected. Faults bordering a graben structure, deep and shallow buried tunnel valleys, glaciotectonic thrust complexes, marine clay units, and sand aquifers are all examples of geological elements mapped by the geophysical data that control groundwater flow and to some extent hydrochemistry. Additionally, the data provide an excellent picture of the salinity distribution in the area thus providing important information on the fresh-saltwater boundary and the chemical status of groundwater. Although, the westernmost part of the study area along the North Sea coast is saturated with saline water and the TEM data therefore is strongly influenced by the increased electrical conductivity here, buried valleys and other geological elements are still revealed. The salinity distribution indicates preferential flow paths through and along specific geological elements within the area. The effects of future sea level rise on the groundwater system and chemical status are discussed with special emphasis on the importance of knowing the existence, distribution and geometry of the mapped geological elements, and assessing their control on the groundwater salinity distribution.

HESSD

9, 2629–2674, 2012

Transboundary geophysical mapping of geological elements

F. Jørgensen et al.

Title Page

Abstract

Introduction

Conclusions

References

Tables

Figures

⏪

⏩

◀

▶

Back

Close

Full Screen / Esc

Printer-friendly Version

Interactive Discussion

1 Introduction

Sea level is predicted to rise in response to climate change (IPCC, 2001) and this will result in saltwater intrusion into coastal aquifer systems based on theory (Bear et al., 1999) as well as observations (e.g. Custodio and Bruggeman, 1987; Iribar et al., 1997; Edmunds et al., 2001; Essink, 2001, 2010). Furthermore, a number of recent studies on current saltwater and freshwater interactions in coastal aquifers demonstrate the increasing problem of saltwater intrusion, globally (e.g. Post and Abarca, 2010). Two recent studies have investigated the impact of sea-level rise on an idealized coastal aquifer system. Chang et al. (2011) show that for confined systems where the ambient recharge to the aquifer remains constant, sea-level rise has no long-term impact on the saltwater wedge. A natural mechanism referred to as the lifting process where the groundwater level increases in response to sea-level rise, has the potential to mitigate the intrusion effects. However, for unconfined systems the lifting process has a lesser influence. The sea-level rise increases the saturated thickness of the aquifer which allows the wedge to penetrate further into the system. Werner and Simmons (2009) further show that the inland boundary conditions are crucial for the effect of sea-level rise on the evolution of the saltwater wedge of unconfined aquifers. For constant flux conditions similar to those used by Chang et al. (2011), where the discharge through the aquifer is assumed to be the same with and without sea-level rise, the wedge do not intrude by more than 50 m for typical aquifer characteristics. However, for head-controlled systems where the inland hydraulic head remain unchanged during sea-level changes, the toe of the saltwater wedge are predicted to migrate hundreds of meters to several kilometres inland for realistic sea-level rise. These studies show the potential impact of sea-level rise for idealized, homogeneous systems.

However, real life geology is newer ideal but characterized by heterogeneity to greater or less extent and it strongly controls saltwater intrusion at the European coastline due to sea level rise during the Holocene (Edmunds et al., 2001). According to Carrera et al. (2010) seawater intrusion is especially sensitive to the sea-aquifer connection, usually associated with the presence of preferential flow paths, a

Transboundary geophysical mapping of geological elements

F. Jørgensen et al.

Title Page

Abstract

Introduction

Conclusions

References

Tables

Figures



Back

Close

Full Screen / Esc

Printer-friendly Version

Interactive Discussion



phenomenon which has been demonstrated also to affect fresh groundwater discharge to the sea (Andersen et al., 2007; Mulligan et al., 2007). A few studies have shown that structural anomalies like fractures, faults and paleo-channels control the saline groundwater movement in some coastal aquifers (Calvache and Pulido-Bosch, 1997; Sprechler, 2001; Yechiely et al., 2001; Mulligan et al., 2007; Nishikawa et al., 2009) or reversely fresh groundwater discharge to or below marine waters as observed in two studies close to the area investigated in this study (Hinsby et al., 2001; Andersen et al., 2007). In Mulligan et al. (2007) the impact of a palaeo-channel breaching a clay layer separating a shallow surficial aquifer from an underlying confined aquifer is studied. Submarine groundwater discharge is found to take place along the margins of the channel whereas seawater inflow occurs along the channel axis. It is found that palaeo-channels should be considered as sites of increased vulnerability to saltwater intrusion. In Nishikawa et al. (2009) a fault system is found to provide a pathway for transport of seawater from a surficial coastal formation to a deeper inland aquifer systems that was otherwise protected by continuous low-permeable layers. Seawater is found to migrate from the shallow deposits into the deeper aquifers through zones near the fault where the discontinuities in the shallow, confining clay layers allow for seawater to move downward. These studies show that it is essential to know the geological architecture of the coastal formations if reliable predictions of seawater intrusion are needed.

A proper 3-D picture of the geology is rarely obtained by borehole data alone. Geophysical methods, such as the seismic reflection method and the transient electromagnetic (TEM) method enables spatially dense collected data giving the needed resolution of vital geological structures (Jørgensen et al., 2003). With the recent improvements of airborne electromagnetics (AEM) (Siemon et al., 2009; Steuer et al., 2009) electromagnetic methods have become even more advantageous within geological and hydrogeological mapping (e.g. Rumpel et al., 2009; Sandersen et al., 2009; Høyer et al., 2011; Teatini et al., 2011). However, borehole geophysics are important data for the corroboration and interpretation of seismic surveys (Rasmussen, 2009; Scharling

Transboundary geophysical mapping of geological elements

F. Jørgensen et al.

Title Page

Abstract

Introduction

Conclusions

References

Tables

Figures



Back

Close

Full Screen / Esc

Printer-friendly Version

Interactive Discussion

et al., 2009) as well as AEM surveys (Mullen and Kellett, 2007) e.g. for separating saline layers from clay layers and for measurements of detailed changes in salinity and lithology profiles at abstraction wells (Buckley et al., 2001).

Airborne systems offer low-cost and fast surveys covering large areas. The systems can be divided into two different types, one in the frequency domain which generally allows for better near-surface resolution than the systems working in the time domain which offer a larger depth of investigation. Very recent developments, however, make airborne TEM capable of significantly improved near-surface resolution (Auken et al., 2010a; Schamper et al., 2012). TEM measures the induced or secondary electromagnetic field due to the diffusion of the eddy currents in the ground after the turn-off of the source current. This inductive response of the ground makes TEM methods well suited for detecting conductive layers where eddy currents are stronger, such as groundwater saturated formations (Auken and Sørensen, 2003; Viezzoli et al., 2010), and even more when saturated with saltwater (Fitterman and Deszcz-Pan, 2004; Auken et al., 2010b; Kafri and Goldman, 2005; Kirkegaard et al., 2011; Kok et al., 2010; Tetini et al., 2011). Clay content also increases the conductivity, making interpretations not straightforward and makes the use of supplementary information from other sources such as well logging necessary (Buckley et al., 2001). Diffusion of the electromagnetic field implies that the resolution capacity decreases with depth, making detailed structures hard to define precisely with TEM data only. Seismic data can give a better resolution of structures, even at great depths. The combined use of TEM and seismic data has shown fruitful results (Jørgensen et al., 2003; Høyer et al., 2011; Teatini et al., 2011), allowing a better estimation of the electrical resistivity with interfaces fixed during the inversion of TEM data (e.g. Nyboe et al., 2010). Also, electrical resistivities determined from AEM can be used to determine the transition between fresh and salt water where no seismic reflector exists (Ribeiro, 2010). However, geophysical well logging is necessary when detailed assessments of the salt/freshwater distribution and estimates of e.g. chloride concentrations at the intake of water supply wells are required (Buckley et al., 2001; Mullen and Kellett, 2007), and for the exact location of lithological boundaries.

**Transboundary
geophysical mapping
of geological
elements**

F. Jørgensen et al.

Title Page

Abstract

Introduction

Conclusions

References

Tables

Figures



Back

Close

Full Screen / Esc

Printer-friendly Version

Interactive Discussion



In this paper we will present the results of a large AEM survey, which combined with seismic data and well logs, provides an excellent picture of a series of subsurface structures as well as the saline/fresh water distribution in the survey area. The influence of these geological structures on the hydraulic system in response to future sea level rise is evaluated. The study emphasizes the need for sound representations of important geological features in numerical models and thus the importance of having geophysical data available.

2 Area description

2.1 Geography

The surveyed area covers the western part of the border region between Denmark and Germany (Fig. 1). The present-day landscape has been shaped by processes during Pleistocene and Holocene time. The morphology is mainly affected by undulating moraine hills preserved from the Saalian glaciations. The Weichselian outwash plains gently dip towards the flat Holocene marshland at the North Sea coast. During the last 8000 yr the marshland has been more or less covered by the North Sea with shallow salt-marsh deposition of mainly marine sand, but peat and gyttja are also present in the up to 10 m thick Holocene succession (Bartholdy and Pejrup, 1994; Hoffmann, 2004). Dike construction during the last 500 yr has converted the area into a dry, drained marshland (Jacobsen, 1964). According to the relief of the landscape, surface water runs off to the marshland from where it is channeled away to the North Sea by a dense net of drainage channels. The entire area has a rural character with cropland and grassland dominating the land use.

2.2 Hydrology and hydrogeology

The marshland is characterized as a low-lying area, which has been developed into farm lands since the 16th century by the development of dikes and later drainage

Transboundary geophysical mapping of geological elements

F. Jørgensen et al.

Title Page

Abstract

Introduction

Conclusions

References

Tables

Figures



Back

Close

Full Screen / Esc

Printer-friendly Version

Interactive Discussion



channels and pumping stations. The surface elevation in large parts of the area is around sea level, Fig. 2. To avoid inundation and make these areas available for agriculture they are drained through the channels. At numerous pumping stations the water collected by the channels are pumped into the Vidaa River which routes the water to the North Sea. Because of the intensive drainage the groundwater level in the upper aquifer do not exceed elevations of approximately one meter below soil surface, corresponding to an elevation equal to or lower than sea level in a large part of the area. Hence, an inland hydraulic gradient is established in a large area under present conditions, which slowly will result in deterioration of the groundwater chemical status.

The salinity in the subsurface of the marshland is generally high and above the WHO/EU drinking water standard of 250 mg l^{-1} , but it varies significantly with depth from about 40 mg l^{-1} to more than 3000 mg l^{-1} (Heck, 1931, 1932; GEUS, 2012; Ødum, 1934). Investigation wells and short wells within the marshland formerly used for households, showed only shallow lenses of freshwater directly resting on brackish groundwater (Ødum, 1934; GEUS, 2012), a situation, which may be compared to the situation in polder areas of Belgium (Vandenbohede et al., 2011) and the Netherlands (de Louw et al., 2011). Hence, groundwater abstraction wells are primarily installed at the margins of the marshland, e.g. the waterworks at the city of Tønder in Denmark and the city of Niebüll in Germany, Fig. 2. The quantity of groundwater abstraction at the well fields is relatively low, approximately 1.5 mill m^3 per year at Tønder and 3.0 mill m^3 per year at Niebüll, respectively, but local depressions in the hydraulic head distribution of the deeper aquifers are observed, increasing the risk of salt water upconing.

2.3 Geology

The geological setting is composed of three major sedimentary sequences. A deep-marine Palaeogene clay is situated at depths of around 300 m in the area (Friborg and Thomsen, 1999). The Palaeogene clay is followed by alternating layers of Miocene sand, silt, and clay. The Miocene section consists of the deltaic Bastrup Formation, the marine clay formations of the fine grained Klittinghoved and the more silty Arnum

**Transboundary
geophysical mapping
of geological
elements**

F. Jørgensen et al.

Title Page

Abstract

Introduction

Conclusions

References

Tables

Figures



Back

Close

Full Screen / Esc

Printer-friendly Version

Interactive Discussion



Formation followed by the fine-grained Gram and Hodde Formations at the top (Rasmussen et al., 2010). The clay formations are intervened by delta lobe sands. The Miocene sequence is covered by a relatively thin sheet of glacial sediments (10–40 m), but in places where tunnel valleys incise the Miocene and Palaeogene, they can be considerably thicker (Thomsen, 1990, 1991; Friberg and Thomsen, 1999; Jørgensen and Sandersen, 2006). The glacial sequence is mainly composed of coarse meltwater sediments, but occasionally, clayey tills and glaciolacustrine clay also occur. A large-scale glaciotectonic thrust complex mapped in the Fanø Bugt is proposed to continue onshore through the survey area (Andersen, 2004). This complex is composed of km-wide structures thrust from easterly directions and with a basal décollement as deep as 200–360 m. Indications of glaciotectonics within the area (at Tønder) are also described on the basis of borehole data (Friberg, 1989). The complex is believed to have formed during the Saalian Warthe glaciations (Andersen, 2004; Houmark-Nielsen, 2007).

Marine Eemian deposits are frequently found in boreholes along the coastal areas in the region (Friberg, 1996; Konradi et al., 2005). The former Eemian shoreline is expected to have been situated more or less along the boundary between the marshland and the Pleistocene upland (Fig. 1). Since many borehole records show marine Eemian in and around the city of Tønder it is proposed that a couple of palaeo-fjords may have reached some kilometres inland here (Friberg, 1996; Konradi et al., 2005).

The survey area is transected by a NW-SE striking fault zone (the Rømø Fault Zone) related to the evolution of the Ringkøbing-Fyn High (Cartwright, 1990). A graben structure (the Tønder Graben) has developed in the area along this fault zone and can be seen within the Palaeogene and Miocene setting (Friberg and Thomsen, 1999). It has been mapped in the survey area on the basis of conventional oil seismic data, but its precise outline and structure is only roughly interpreted. A generalized stratigraphical log for the area is shown in Fig. 3.

**Transboundary
geophysical mapping
of geological
elements**

F. Jørgensen et al.

Title Page

Abstract

Introduction

Conclusions

References

Tables

Figures

⏪

⏩

◀

▶

Back

Close

Full Screen / Esc

Printer-friendly Version

Interactive Discussion



3 Methods

3.1 SkyTEM

The SkyTEM system initially developed by Sørensen and Auken (2004) is a helicopter-borne time domain AEM system which consists of a wire loop transmitter of several hundred square meters and of a small receiver loop of less than 1 m² (Fig. 4). Different sizes of the transmitter loop exist depending on the depth of investigation required for a survey. The intensity of the current as well as the number of turns can also be increased to amplify the magnetic moment, and so to improve the signal-to-noise ratio and get a larger depth of investigation. However, there is a trade-off since higher current will induce a longer turn-off of the current inside the loop, which prevents the use of early times resulting in a poor near-surface resolution. For this reason SkyTEM usually measures with two moments, one called Super Low Moment (SLM) which gives information of the near surface, and one called High Moment (HM) which gives deep information. These two moments are jointly inverted for each single sounding estimating electrical resistivity from the near-surface to a depth of 250–300 m, depending on the setup used and the geology in the survey area (Fig. 4). To ensure corrections due to the movements of the frame, the height (about 30 m) and the pitch/roll are continuously measured by lasers and by inclinometers, respectively (Auken et al., 2009). With a nominal speed of 45 km h⁻¹ and good weather conditions, the SkyTEM system has a production rate of 1000 km of flightlines within 4–5 days.

3.2 Seismics

Seismic methods utilize differences in mechanical properties of geological units. The propagation velocity and signal strength of seismic waves inside the earth depend on the dynamic elastic constants of the rocks and on their density. The method provides primarily information about the framework and delineation of geological units. Different types of waves are nowadays used for near surface seismic surveying: compressional

Transboundary geophysical mapping of geological elements

F. Jørgensen et al.

Title Page

Abstract

Introduction

Conclusions

References

Tables

Figures

⏪

⏩

◀

▶

Back

Close

Full Screen / Esc

Printer-friendly Version

Interactive Discussion



or *P*-waves and shear or *S*-waves. Both differ in depth range and resolution. Due to low velocity or impedance contrasts in the low consolidated Quaternary or Neogene sediments present in the surveyed area, the refraction seismic method is not suitable. The reflection seismic systems used in this paper are appropriate for the target depths of 20 m to 700 m. The depth penetration is realizable with vibro seis and the common midpoint (CMP) method. With the *P*-waves used the resolution of depth-and-interval geology (Steeple, 2005) is in the size of 4 m depending of wavelength and depth of target.

3.3 Borehole geophysics

A large number of different types of logging probes exist for measurements in boreholes. The different probes typically measures changes in physical characteristics of the surrounding formation, which reflects changes in lithology and/or porewater salinity. The use of a combination of different geophysical logging probes such as gamma (NG), induction (IN) and fluid temperature and conductivity (FTC) have proved very efficient for investigations of important characteristics of coastal aquifer systems (Buckley et al., 2001). These tools have therefore been used in the present study. The NG and IN tools reveal changes in the lithology of the formation surrounding the wells, while the FTC probe measures the temperature and electrical conductivity of the water inside the borehole, which generally represents an average of the conductivity of the porewater in the formation around the screened part of cased wells. Besides changes in the lithology of the formation the IN logging probe also record detailed changes in the salinity of the porewater in the formation around the well or rather a combination of changes in porewater hydrochemistry and formation lithology.

Transboundary geophysical mapping of geological elements

F. Jørgensen et al.

Title Page

Abstract

Introduction

Conclusions

References

Tables

Figures



Back

Close

Full Screen / Esc

Printer-friendly Version

Interactive Discussion



4 Surveys performed

4.1 SkyTEM

A first survey was carried out in the German part north of the town of Leck on 17–25 September 2008 (Fig. 5). This survey consists of 1481 line km with a line spacing of 250 m and covers an area of 396 km². The second survey was made in the Danish part around the town Tønder on 1–21 April 2009. This survey includes 1750 line km with a main line spacing of 166 m and covers an area of 325 km². The SkyTEM survey utilized the largest SkyTEM loop with an area of 494 m² and a maximum current for the HM of 95 A, resulting in a large penetration depth compared to other SkyTEM systems with smaller loops and lower currents. With a speed of 72 km h⁻¹ for the Leck survey and a speed of 43 km h⁻¹ for the Tønder survey, the average lateral resolution along the flight lines is about 25–30 m at least for the first tens of meters. The resolution then decrease along with the diffusion of the electromagnetic signal towards the depth.

The data have been processed and inverted with the Aarhus Workbench software package (Viezzoli, 2009; Roth et al., 2011). The first step in the processing of the raw data is the removal of all coupling effects induced by man-made installations, such as power lines, cables, pipes, or railroads (Sørensen et al., 2001). Since these coupling effects can not be modelled and compensated, parts of flight lines affected by these couplings have to be removed from the data set. While automatic filtering can remove some of them, a careful manual check has to be undertaken to remove both undetected couplings and remnants of only partly removed couplings. Once the couplings have been removed from the raw data, the data are averaged with trapezoid filters whose width increases as the time after the turn-off of the source increases, i.e. as the data contain deeper and deeper information. These trapezoid filters are set in such a way that they are adapted to the signal-to-noise ratio which decreases at late times. Finally, late time data are removed from averaged data where the background noise level reaches the level of the earth response. Other filters on the altitude and the pitch/roll of the loop are also applied since these parameters influence the strength of the recorded signal.

Transboundary geophysical mapping of geological elements

F. Jørgensen et al.

Title Page

Abstract

Introduction

Conclusions

References

Tables

Figures

⏪

⏩

◀

▶

Back

Close

Full Screen / Esc

Printer-friendly Version

Interactive Discussion



**Transboundary
geophysical mapping
of geological
elements**F. Jørgensen et al.

[Title Page](#)[Abstract](#)[Introduction](#)[Conclusions](#)[References](#)[Tables](#)[Figures](#)[⏪](#)[⏩](#)[◀](#)[▶](#)[Back](#)[Close](#)[Full Screen / Esc](#)[Printer-friendly Version](#)[Interactive Discussion](#)

After a final review of the data to check that all couplings have been removed, the data are then inverted through a Spatially Constraint Inversion algorithm which gives a quasi-3-D interpretation of the ground (Viezzoli et al., 2008, 2009). In this inversion procedure the parameters of soundings are linked together with constraints which are proportional to the distance separating them. These constraints prevent artificial local results which may be due to poor signal-to-noise ratio and to poorly defined parameters. However, care has to be taken when setting the strength of these lateral constraints which can induce too smoothed geological structures. For more realistic interpretation and to avoid problems due to a fixed number of layers, the sections are inverted into smooth models with 19 layers. The thicknesses of these are fixed and increase logarithmically with the depth, and their resistivity values are linked by vertical constraints to ensure smooth variations between the layers of the same sounding.

4.2 Seismics

On the German border side LIAG (Leibniz Institute for Applied Geophysics, Hannover) accomplished a *P*-wave seismic reflection survey in May 2009. This was recorded with conventionally planted z-Geophones (SM4 20 Hz) and LIAG's vibrator truck in the area near Süderlügum (Fig. 6). Geometry of 5 m receiver spacing and 10 m source spacing emerge a high resolution underground image with 2.5 m common-midpoint (CMP) distance. For acquisition LIAG used up to 264 channels in a combination of split spread and roll along technique, which qualified in previous surveys. Source-receiver offsets range from –1200 m to +1200 m. The maximum CMP fold is 129; the mean fold is at least 60. The hydraulic vibrator truck MHV2.7 (2.7 ton vibrator) was controlled by a sweep of 30 Hz–200 Hz with a length of 10 s and 4 sweeps were vertically stacked at each source point. The data were recorded with Geometrics Geode system and saved in stacked and correlated state. For quality control several records with an impulse source (hammer blow) were taken. In total 817 vibrator points on 7.8 km of profile were recorded within 8 days. Five individual profile sections were acquired (G1–G5).

On the Danish side of the border five seismic reflection profiles were also surveyed (D1–D5). The profiles cover a total distance of 29.5 km and were recorded in April and May 2010 using an IVI Minivib T7000 3.5 ton vibrator and 224 towed 14 Hz L10 AI geophones in groups of two. The first group was used for recording the “pilot-trace” of the vibrator. The geophone trail wire length was 225 m. The first 49 active geophone groups were mutually separated by 1.25 m while spacing between each of the remaining 63 groups was 2.5 m. The source (vibro point) spacing was 10 m with a distance to the first active geophone group was 6.25 m. Acquisition was conducted by use of Geometrics Seismodule Controller software and a 64 channels Geometrics StrataVisor instrument supplemented by two 24 channels Geometrics Geode recording units. At each source point a minimum of two vibrator sweeps of 40–400 Hz with a length of 10 s were carried out. The data were collected and processed by Rambøll (2010).

The collected raw data show varying quality. The survey in the vicinity of Süderlügum profiles G1, G3 and G4 show a good signal/noise ratio, while profiles G2 and G5 were located near main roads and were influenced by car generated noise. The profiles north of the border were all located on roads with limited amount of traffic and the sections were therefore only to a minor extent influenced by traffic generated noise. On the other hand strong winds prevailing in the area were probably part of the reason for a lack of quality on two profiles, D1 and D5. These two profiles were therefore resurveyed. Unfortunately only D1 did benefit by the effort. After geometry assignment first breaks were picked and controlled with first breaks from impulse source. Refraction statics were calculated from the first break picks and applied in the pre-stack processing. Additional steps were amplitude control by automatic gain control, spectral whitening and bandpass filtering as well as trace muting and application of residual statics. Velocity analysis provides stacking velocities for dip move-out (DMO) and normal move-out (NMO) correction and following CMP stacking created seismic time sections. In the post-stack processing finite difference time migration removed diffractions and F-X deconvolution smoothed the resultant section. Time-to-depth conversion finally created the depth section, which are used for interpretation. Stacking

**Transboundary
geophysical mapping
of geological
elements**

F. Jørgensen et al.

[Title Page](#)[Abstract](#)[Introduction](#)[Conclusions](#)[References](#)[Tables](#)[Figures](#)[⏪](#)[⏩](#)[◀](#)[▶](#)[Back](#)[Close](#)[Full Screen / Esc](#)[Printer-friendly Version](#)[Interactive Discussion](#)

velocities were converted into interval velocities and for time-to-depth conversion an averaged single interval velocity function was used.

4.3 Borehole geophysics

Three deep boreholes were investigated by logging probes in the study area, one well in Germany (A49-3, north of Karlum) and two in Denmark (archive no. 166.711 and 167.1538; GEUS, 2012). See Fig. 6 for locations. Two of the wells (A49-3 and 166.711) were investigated by the use of a combination of different geophysical logging probes including natural gamma (NG), induction (IN) and fluid temperature and conductivity (FTC). The logs were run at a speed of 3 m min^{-1} in either downwards (NG, FTC) or upwards direction (IN). The third well (167.1538) were logged in an open hole with drilling mud fluids, hence the fluid conductivity log does not measure the porewater conductivity.

By using Archie's law (Archie, 1942), it is possible to calculate the formation factor (the ratio between formation and porewater resistivity) from measurements of formation resistivity (by IN logs) and fluid resistivity (by FTC logs) through the screened section of a borehole. The formation factor is important when developing maps that provide a "regional" overview of the variations of the groundwater resistivity (or conductivity) and e.g. assessments of groundwater chloride concentrations and chemical status in the investigated area.

It is important to note that observed changes in formation resistivities may be the result of changes in either formation lithology or porewater salinity (or both) e.g. a decrease in the IN log may be due to either increasing clay contents or increasing porewater salinity. The only way to assess the relative importance of these is by use of the NG log, as the NG log are not affected by changes in porewater salinity, or by taking lithological information from sample descriptions into account. Hence, lithological descriptions of borehole samples or the NG logs are important for correct interpretation of both IN logs and AEM measurements, and hence the distribution of saltwater and the development of salt/freshwater interfaces in coastal aquifer systems.

**Transboundary
geophysical mapping
of geological
elements**

F. Jørgensen et al.

Title Page

Abstract

Introduction

Conclusions

References

Tables

Figures

⏪

⏩

◀

▶

Back

Close

Full Screen / Esc

Printer-friendly Version

Interactive Discussion



5 Results

5.1 Data interpretation

After processing and inversion the geophysical data have been subjected to geological interpretation. In order to transfer the acoustic and resistivity data into lithology and to establish a spatial conceptualisation of the geological structures and elements of the subsurface, borehole data is a vital constituent. Most borehole data originate from water well construction, but also a few investigation drillings contribute to groundtruthing of the geophysical data. The available sample descriptions vary in quality and care must be taken when used within the process of geological interpretation. Generally, they should be supported by geophysical borehole logs whenever possible. Furthermore, most of the boreholes are not very deep, typically less than 25–50 m, and they are too widely spaced to follow the spatial variations in the subsurface. The seismic data contribute with detailed structural information along the 2-D sections, but again, even when combined with borehole data, there is no correlation between the sections in the area. The seismic data are displayed with borehole data (if deep boreholes are available within a reasonable distance from the section) and transparent colour-scaled SkyTEM data on top, Fig. 7. This enables the interpreter to compare the structural information from the seismic data with the direct and derived lithological information from boreholes and SkyTEM.

The SkyTEM resistivity data is converted to a series of horizontal slices each representing mean values in intervals of 5 m. Resistivity values in these intervals are calculated for each SkyTEM smooth layer sounding model and subsequently interpolated using kriging, with a cell size of 100 m. In order to inspect the resistivity data spatially in detail, all grids from 250 m below sea level (m b.s.l.) to surface are stacked into a 3-D resistivity volume. This 3-D resistivity volume can be sliced horizontally at different levels (Figs. 8 and 9), but also vertically either along the seismic sections (Fig. 7) or along every desirable profile section through the area Fig. 10.

Transboundary geophysical mapping of geological elements

F. Jørgensen et al.

Title Page

Abstract

Introduction

Conclusions

References

Tables

Figures



Back

Close

Full Screen / Esc

Printer-friendly Version

Interactive Discussion

During the process of geological interpretation it is essential not only to evaluate interpolated resistivity data, because basic geophysical information is often lost in the transformation from sounding data to interpolated grids. The inverted resistivity models, db/dt data, and data uncertainty must regularly be individually consulted in order to avoid misinterpretations due to noise, equivalence effects, resolution issues, structural heterogeneity, etc.

A series of prominent geological features claimed to be decisive in relation to future potential saltwater intrusion, will in the following be outlined and described on the basis of the combined geophysical data set.

5.2 Faults

Faults related to the NW-SE striking Rømø Fault Zone are clearly seen in the seismic profile D4 (Fig. 7). Two normal faults with offsets of 50–100 m are present on the section. These faults bound a graben structure (the Tønder Graben) and intersect the entire setting until at least the Miocene. The Miocene Gram and Hodde clay (see section below) is subsided into the graben structure and the faults must therefore have been active during or after the deposition of this clay. The southernmost fault seems to terminate into an incised tunnel valley (see section below) and the valley is therefore formed after the formation of the graben structure. The faults can also be laterally delineated in the resistivity data since the down-faulted Miocene clay is very electrically conductive. The clay layer is therefore distinct in the seismic section D4 (Fig. 7) and seen as a 75 m thick low-resistive layer (8–10 Ωm) in the graben structure. By slicing the 3-D resistivity grid horizontally at levels around the subsided clay (100 to 175 m b.s.l.) the graben structure is delineated laterally by a low-resistive elongated body (Fig. 8). The extent of the northern fault can also be traced in resistivity slices at higher levels (Fig. 9). An example of a S-N vertical slice through the 3-D resistivity volume is shown as Profile 1 in Fig. 10. The faults bounding the graben structure are also clearly seen here (between profile coordinates 13 750 m and 16 000 m).

Transboundary geophysical mapping of geological elements

F. Jørgensen et al.

Title Page

Abstract

Introduction

Conclusions

References

Tables

Figures

⏪

⏩

◀

▶

Back

Close

Full Screen / Esc

Printer-friendly Version

Interactive Discussion



5.3 Palaeogene and Miocene

Interpretation of oil seismic data has shown that the surface of the Palaeogene clay is generally situated at depths between 250 and 320 m b.s.l. outside the Tønder graben and inside the graben it reaches depths of about 450 m b.s.l. (Friborg and Thomsen, 1999). A deep borehole (archive no. 167.1538; GEUS, 2012) situated exactly on the seismic section D4 (Fig. 7) show that the top of the Palaeogene is situated at 325 m b.s.l. corresponding to a high amplitude reflection on the seismic section denoted by a blue line. The clay was found in the borehole samples and the exact location was confirmed by the NG log. This reflection can be traced on each of the seismic lines collected in the area. The reflection reaches depths of more than 500 m b.s.l. within the graben on section D4. The depth to the Palaeogene is generally too large to be resolved by the SkyTEM soundings. However, where it reaches the highest levels, towards the North and East, it is resolved as a very conductive layer (Fig. 10, Profile 2). In these areas it reaches about 200 m b.s.l.

The Miocene sequence is primarily seen in the SkyTEM resistivity data as an upper conductive layer (8–10 Ωm) and a lower resistive layer (>100 Ωm). The upper layer, which is 50–75 m thick, is composed of marine Gram and Hodde clay and occurs in areas where the glaciers did not remove or disturb it (buried valleys and glaciotectonics, see below). Where preserved, it is clearly portrayed in both the vertical sections, Profile 1 and 2, Fig. 10. The layer is situated at levels of about 50 to 100 m b.s.l. in the eastern part, whereas it apparently gradually dips towards the West to a level of 100 to 150 m b.s.l.

The lower, resistive layer is mapped where the SkyTEM system is able to penetrate the Gram and Hodde clay layers (Fig. 10). According to Rasmussen et al. (2010) the less clayey marine Arnum Formation should be present below the Gram and Hodde clay in the survey area, followed by the deltaic sandy Bastrup Formation. The widespread high-resistive Miocene layers in the area (Figs. 7, 9 and 10) are most likely corresponding to sandy members of Bastrup Formation.

**Transboundary
geophysical mapping
of geological
elements**

F. Jørgensen et al.

Title Page

Abstract

Introduction

Conclusions

References

Tables

Figures



Back

Close

Full Screen / Esc

Printer-friendly Version

Interactive Discussion



5.4 Tunnel valleys

The area is dissected by a series of both deep and more shallow incisions that in appearance and property are typical for buried tunnel valleys in the area (Jørgensen and Sandersen, 2006, 2009). The deepest tunnel valley is seen on the two seismic sections D2 and D4 (Fig. 7). This valley reaches about 350 m b.s.l. but other valleys are much shallower. The valleys are precisely delineated in the resistivity data (Fig. 9) because the resistivity of the infill typically differs from the surroundings. In some situations they are filled with either glaciolacustrine clay or clay till and if incised into sandy Pleistocene or Miocene sediments they occur as elongated low-resistive structures. In other situations they are filled with coarse glaciofluvial deposits and in such cases they occur as resistive structures. The valleys are typically visible at different levels along their pathways (Fig. 9). Their widths vary between a few hundred meters to about 2.5 km. As mentioned, the infill is composed of a variety of Pleistocene sediments. Profile D2 (Fig. 7) show thick high-resistive sediments in the lower part of the valley covered by a 25 to 50 m thick layer of low-resistive sediments. Above this, high-resistive sediments are found again and the entire setting is capped by a thin low resistivity layer. According to the borehole 166.711 (lithology and IN log, Fig. 7) the high resistive sediments correspond to glacial meltwater sand whereas the low-resistive layer corresponds to glaciolacustrine clay and silt. The low-resistive top layer corresponds to clay till. Approximately the same overall setting is seen in the same valley in Profile 1 (Fig. 10, profile coordinate 9500–11 500 m). The valley is also crossed by section D4, but here the drilling (167.1538) show a much thicker sequence of fine-grained meltwater sediments (Fig. 7). The IN log, however, indicates that the upper parts of this sequence are more resistive and are therefore likely to be more silty than the lower part. A distinct drop in formation resistivity to about 5 Ω m is seen for the lower part of the valley sediments in the IN log. Since the sediments are mostly described as sandy at this level the formation must be affected by saline porewater here. This corresponds to the low resistivities as measured by the SkyTEM (Fig. 7).

Transboundary geophysical mapping of geological elements

F. Jørgensen et al.

Title Page

Abstract

Introduction

Conclusions

References

Tables

Figures

⏪

⏩

◀

▶

Back

Close

Full Screen / Esc

Printer-friendly Version

Interactive Discussion



The deep valleys typically cut through the Miocene clay layers and into the deep sandy Miocene layers (Figs. 7 and 10) and they do not follow the fault structures and therefore seem to be unaffected by the presence of these (Fig. 8).

All boreholes hosted in the Danish national borehole database (GEUS, 2012) have been searched for records of Eemian deposits throughout the area, and boreholes with hits are plotted on the uppermost horizontal slice in Fig. 9. It appears that there is a good match between the outline of one of the buried valleys and the occurrences of Eemian deposits. It is likely that this particular valley was open and inundated by the sea during the last interglacial. The mapped valley therefore constitutes one of the palaeo-fjords proposed by Friberg (1996) – the Tønder Fjord. On top of the marine Eemian the valley is filled by meltwater sediments from the Weichselian glaciation (Konradi et al., 2005) and it is therefore not visible in the present-day topography. The precise time of incision of the valley is uncertain but a Saalian age is likely, since it was open during the Eemian. The age of the other valleys is unknown, but at least the deep valley seen on Profile D2 and D4 (Fig. 7) is possibly older than the Late Saalian, because it is situated below the Saalian moraine hill north of Tønder (Fig. 1) which is covered by Late Saalian till.

The general pattern of the valleys indicates more than one single valley generation. There seem to be NE-SW oriented valleys, N-S oriented valleys and one SE-NW oriented valley – probably three generations.

5.5 Glaciotectonics

The SkyTEM data show a very heterogeneous picture in two distinct areas (Fig. 9). These areas are situated in the central northern part and in the central southern part of the survey area. The areas appear generally as more resistive but they are interrupted by many small, often slightly elongated low-resistive bodies. The seismic lines D2 and G1–4 both collected in the areas with a heterogeneous appearance in the resistivity image indicate the presence of folds and thrust structures with a décollement between 150 and 200 m b.s.l. It is therefore inferred that the heterogeneous areas express the

Transboundary geophysical mapping of geological elements

F. Jørgensen et al.

Title Page

Abstract

Introduction

Conclusions

References

Tables

Figures



Back

Close

Full Screen / Esc

Printer-friendly Version

Interactive Discussion



extent of one or two large glaciotectonic complexes. The elongated low-resistive bodies seen in the resistivity data are mainly oriented SE-NW indicating an ice movement from a northeasterly direction. This is more or less consistent with the findings in the Fanø Bugt, where the large glaciotectonic complex was formed by a glacier from the East (Andersen, 2004). Therefore, it is plausible that the complexes found in our survey is an onshore continuation of the larger offshore complex as also proposed by Andersen (2004). If this is true, and the assumed Late Saalian age of the complex is true, then at least the deep buried tunnel valley depicted on the seismic sections D2 and D4 (Fig. 7) which is older than this, must have been exposed to the glaciotectonic stress. Structures which could represent glaciotectonic deformation within the valley fill especially between 2000 and 3000 m on Profile D4 and 2500 and 3500 m on Profile D2 can be traced (Fig. 7) but this interpretation is uncertain. On the other hand, a relatively clear erosional boundary between the valley and the surroundings indicates that the valley infill was not severely deformed by glaciotectonic deformation.

On the seismic Profile G1–4 there are indications of an old incision below the décollement plane (Fig. 7), showing the pre-existence of a valley before the glaciotectonic deformation took place. Thus, the exact chronology of valley incision and glaciotectonic deformation is difficult to assess. But it seems likely that valley incision not only took place after the deformation phase but also before.

5.6 Formation resistivity, formation factors, and groundwater salinity and chemical status

The saltwater saturated subsurface of the low-lying marshland is clearly depicted in the resistivity data, which generally shows low resistivities here. The area with low resistivities in the southwestern part of the survey area (as seen in Fig. 9, 32.5 m below sea level) corresponds to the extent of the marshland (Fig. 1). Although the setting is saturated with saltwater it is still possible to delineate the buried valleys and the Miocene layers in the maps and on the cross sections (Figs. 9 and 10, Profile 2). The resistivity of the Miocene silt/sand is seen to be considerably lower than in the

Transboundary geophysical mapping of geological elements

F. Jørgensen et al.

Title Page

Abstract

Introduction

Conclusions

References

Tables

Figures

⏪

⏩

◀

▶

Back

Close

Full Screen / Esc

Printer-friendly Version

Interactive Discussion



freshwater saturated areas, but the exact resistivity value that deep in the conductive setting, which acts as an effective shield, is not possible to assess due to resolution problems. The resistivity of the assumed Miocene clay is somewhat lower (3–5 Ωm at profile coordinate 0–14 000 m Profile 2, Fig. 10) than it is in the freshwater saturated setting (5–7 Ωm), and the contrast to the bounding sediments above and below is still preserved.

Above the Miocene clay layer in the saltwater saturated area (Fig. 10, Profile 2) the setting can generally be subdivided into three layers based on the resistivity. Right above the assumed clay there is a layer with a relatively high resistivity, although it is still rather low ($\sim 6\text{--}8\ \Omega\text{m}$). Then a low-resistive layer follows ($\sim 2\text{--}4\ \Omega\text{m}$) topped by a shallow near-surface layer (0–10 m depth) with sometimes relatively high resistivities. The last layer's high-resistive spots are probably identical to the areas with shallow lenses of freshwater and old drinking water wells. The resistivity of the second layer is higher than expected for sediments saturated by seawater originating from the North Sea. The formation factor is estimated for the wells 166.711 and A49-3 to be 3.5 and 3.1, respectively, for the screened sandy sections of the wells. This compares well with the average formation factor (3.4, std. 0.5) estimated from 19 well logs in coastal sandy aquifers in Belgium, The Netherlands, Germany and Denmark performed as part of the CLIWAT project and from assessments of the average formation factor (3.5) in sandy aquifers at the Belgian coast line (Vandenbohede et al., 2011). With a typical resistivity for seawater of $0.3\ \Omega\text{m}$, the resulting formation resistivity would be approximately $1.0\ \Omega\text{m}$ (Archie, 1942). A resistivity of $1\ \Omega\text{m}$ has been found in a borehole log from the Northern part of the island of Rømø (archive no. 148.52) in the Northern part of the Wadden Sea in a previous study (Hinsby et al., 2001) and true seawater salinities were confirmed by chemical groundwater analyses at the relevant level. Since the resistivity is as high as 6–8 ohmm in the investigated area, the sediments does not seem to be saturated with fully marine sea water. The same reasoning applies for the Miocene clay layer and the upper low-resistive layer. These do not reach that low resistivity values either, and the sediments are therefore not saturated with fully marine sea water. A

**Transboundary
geophysical mapping
of geological
elements**

F. Jørgensen et al.

Title Page

Abstract

Introduction

Conclusions

References

Tables

Figures

⏪

⏩

◀

▶

Back

Close

Full Screen / Esc

Printer-friendly Version

Interactive Discussion



couple of flight lines over the tidal flat on the seaside of the dike also show resistivity values above the expected for sediments saturated by fully marine water (Fig. 9).

Assuming an average formation factor of 3.5 the porewaters of the sandy aquifers in the region breach the EU drinking water guideline for electrical conductivity (250 mS m⁻¹ = 4 Ωm), when the AEM and/or borehole log measurements show formation resistivities below 14 Ωm (3.5 × 4 Ωm). Similarly, in analogy with a suggested European threshold value for chloride (Hinsby et al., 2008) the threshold value for electrical conductivity would be 150 mS m⁻¹ or 23 Ωm (3.5 × (1/0.15)). Hence, sandy aquifers in the investigated region with resistivities less than approximately 23 Ωm contain groundwater of poor chemical status according to the EU groundwater directive.

6 Hydrogeological evaluation and discussion

The results from the survey show that large parts of the area are affected by saltwater. The origin of the saltwater observed in the Miocene aquifers might be residual saltwater from the time when the formation was deposited, saltwater flushed into the system during Pleistocene or Holocene transgressions, or saltwater intruded during recent time after dike construction and drainage of the marshland. Since saltwater is not found in the Miocene sediments neighbouring the marshland it is, however, likely that the residual saltwater have been flushed by freshwater during periods with sea levels much lower than the present, e.g. during the Last Glacial Maximum where the sea level was more than 120 m lower than the present (Edmunds et al., 2001; Clark and Mix, 2002). Therefore, the origin of the saltwater is expected to be more recent, either caused by infiltration and intrusion during the Holocene transgression or/and as a result of seawater intrusion after the drainage of the area. Based on the current knowledge, however, it is difficult to make further estimates on the origin of the saltwater. The dynamics of the saltwater is also difficult to assess, i.e. if residual saltwater is presently being flushed by freshwater or if the present drainage and pumping

Transboundary geophysical mapping of geological elements

F. Jørgensen et al.

Title Page

Abstract

Introduction

Conclusions

References

Tables

Figures

⏪

⏩

◀

▶

Back

Close

Full Screen / Esc

Printer-friendly Version

Interactive Discussion

in the area generates additional saltwater intrusion to the aquifers. However, the low resistivities seen on Fig. 10, Profile 2, between coordinates 0 and 12 000 m indicates that flushing of the saltwater is not taking place or is very low in the current situation. Only the uppermost about 10 m show spot wise high resistivities indicative of shallow freshwater lenses situated above the saltwater system. Saline groundwater is however expected to seep into the drainage channels, either as upward flow below the drainage channels or at the interface between the rainwater lens and the saline groundwater below (de Louw et al., 2011).

The resistivities of the formations in the marshland area, Fig. 10, Profile 2, are as mentioned higher than expected for sediments saturated with fully marine water. Hence, the salinity of both the Miocene clay and the sandy Miocene and Pleistocene deposits above is below that of the North Sea indicating that dilution has taken place. Such conditions have also been reported from Rømø where partly flushed seawater (brackish water) was also found at a depth of 300 m and below more than 100 m of marine clays in well 148.52 (Hinsby et al., 2001). Due to density differences rainwater from above is not expected to recharge deep into the profile. The reduced salinity may therefore be caused by upward flow of fresher water from below. Active groundwater flow may take place from east to west through the deep Miocene sediment seen on Fig. 10, Profile 2 between coordinates of 0 and 14 000 m at elevations below -150 m. This aquifer is probably fed by groundwater recharging in the central part of Jutland (Hinsby et al., 2001) and is known to be an artesian aquifer. Unfortunately, measurements of hydraulic head from the deep part of the Miocene aquifer are only available at a few locations, including archive no. 158.698 and 159.995 (GEUS, 2012) located 15 km north and 14 km north-east of Tønder, respectively, where head values above soil surface have been observed. The hydraulic heads of this formation may therefore be higher than the equivalent freshwater heads of surficial sandy formations intruded by sea water and in this case groundwater is expected to seep up through the clay layer and further up through the sand layer due to buoyancy forces. Such a mechanism could give rise to salinities that are lower than those corresponding to fully marine conditions

**Transboundary
geophysical mapping
of geological
elements**

F. Jørgensen et al.

Title Page

Abstract

Introduction

Conclusions

References

Tables

Figures

⏪

⏩

◀

▶

Back

Close

Full Screen / Esc

Printer-friendly Version

Interactive Discussion



and result in the observed elevated resistivities. The existence of an active flow system in the lower Miocene sand/silt formation could furthermore explain the relatively high resistivities found in the deeper parts of the buried valley seen on Fig. 10, Profile 2 between coordinates 1000–1500 m and in Fig. 8 at a depth of 152.5 m. The existence of fresh water below the more saline water in the valley probably requires that (1) the infill of the valley is layered such that the lower part is partially confined from the upper saline part and (2) that the flux of fresh groundwater through the lower part is sufficient to dilute the buoyancy driven downward flux of high salinity water from above. If these requirements are fulfilled the buried valley might act as a drainage channel for the deep Miocene aquifer. This hypothesis is corroborated by the fact that the Miocene sand formations tend to pinch out close to the west coast of Jutland (Scharling et al., 2009) in which case the flow through the formations is restricted. However, as the layered Miocene sequence seems to have been destroyed by the formation of the glaciotectonic complex just to the east of the marshland (Fig. 10) the Miocene clay may not be very effective as a confining layer in this area. The hypothesis discussed above is therefore only tentative and requires that the confining layer is uninterrupted, also by other elements such as tunnel valleys.

Low resistivities likely to represent saline groundwater are also found on Profile 1 (Fig. 10) between coordinate 6000 and 7000 m next to the marshland. Here they are found in the Miocene silt/sand at a location exactly below one of the tunnel valleys that perforates the Miocene clay. This area was not inundated by the Holocene transgression, but the tunnel valley was an open fjord during the Eemian (Fig. 9) and the saline groundwater may have infiltrated through the valley to the underlying Miocene sand and silt layers during this period. If seawater intruded through the valley during the Eemian there should be no groundwater flow in the aquifer, since the seawater body still exists. This contradicts to the hypothesis discussed above, where flow was expected to take place in the lower Miocene aquifer. Another possibility is therefore that the valley is deeper than anticipated from the SkyTEM data (as drawn on Fig. 9) and that the observed low resistivities originate from clay sediments and/or saltwater within the valley

**Transboundary
geophysical mapping
of geological
elements**

F. Jørgensen et al.

Title Page

Abstract

Introduction

Conclusions

References

Tables

Figures

⏪

⏩

◀

▶

Back

Close

Full Screen / Esc

Printer-friendly Version

Interactive Discussion



itself. If the latter is true and the valley hosts saltwater, the water could perhaps have intruded laterally from the North Sea through the valley infill. Unfortunately, there are no boreholes, logs or seismic data to clarify this question.

The continuation of the tunnel valleys towards the North Sea through the marshland is evidenced as elongated bodies with resistivity values that are generally slightly lower than their surroundings (Figs. 9 and 10). In the uppermost 60 m the south westward continuation of the above-mentioned Eemian valley exposes resistivities in the vicinity around 2–3 Ωm and in the south westernmost part close to the North Sea it is between 1 and 2 Ωm . Thus, unlike the surrounding sediments, the valley may here host full marine water. This water could be remnants of old marine water, but could also here point to the fact that the valleys act as pathways for past and/or present seawater intrusion into the marshland.

As described above the hydrogeology of the study area is very complex and detailed predictions of the impact of sea level rise are therefore difficult to make. The complex geological setting and hydrological flow system only make tentative evaluations possible. Due to the drainage system in the marshland the groundwater table is here located close to or below sea level. Hence, a hydraulic gradient from the sea towards the inland areas exists at present conditions. Saltwater is therefore expected to migrate into the inland aquifers. Since the groundwater table is controlled by the drainage and pumping systems, a rise in sea level will not affect the elevation of the groundwater table in the marshland. Hence, a higher sea level is expected to result in a higher gradient and therefore increasing saltwater intrusion (Werner and Simmons, 2009) at least in the upper aquifers. Hansen et al. (2011) show that in the border region of Denmark and Germany isostatic down-warping at a rate of 0.25–0.50 mm yr^{-1} takes place. In combination with eustatic sea level rise this makes the area especially vulnerable to sea water intrusion.

If the geology in the area was not interrupted by several structural anomalies including the fault system, the buried valleys and the glaciotectonics, the relative thick and widespread Miocene clay layer would be continuous and cover a large area from

**Transboundary
geophysical mapping
of geological
elements**

F. Jørgensen et al.

Title Page

Abstract

Introduction

Conclusions

References

Tables

Figures



Back

Close

Full Screen / Esc

Printer-friendly Version

Interactive Discussion



central Jutland into the North Sea. In this case the aquifer in lower Miocene sand/silt (Fig. 10) would be confined and would presumably not be intruded by seawater as it would be protected by the overlying clay layer. However, the geological anomalies do provide pathways between the upper Quaternary aquifers and the Miocene aquifers in the area as sea-aquifer exchange usually takes place along preferential pathways (Carrera et al., 2010). Density-driven convective flow may take place at these locations resulting in saltwater intrusion into the deeper aquifers. Head gradients caused by groundwater abstraction from the Miocene aquifers, e.g. at Tønder and Niebüll may enhance this development. An example is seen at the Tønder Graben where it is likely that the upper aquifers is in hydraulic contact with the lower Miocene aquifer (Figs. 8 and 10) and therefore may serve as a pathway for saline water in the area close to the sea. A similar situation has been described by Nishikawa et al. (2009). The glaciotectonic complex seen on Fig. 10, Profile 2 may constitute another structure where downward migration of saltwater may take place if sea water intrudes further in the upper aquifer, e.g. at coordinates 12 000–14 000 m.

Even more critical for the exchange of saline groundwater between aquifers may be the frequent occurrence of incised and cross-cutting buried tunnel valleys (Figs. 7, 9 and 10). The east-west aligned buried tunnel valleys connecting the sea aquifers and the Miocene aquifers through the marshland as well as further inland constitute central elements for the horizontal exchange of water. They often contain coarse-grained and high permeable infills allowing for immense vertical exchange between the upper and the lower Miocene sand layers. Since the valleys cross-cut and since they often contain more than one aquifer (like the deep valley shown in Fig. 7) exchange may also take place between different valley aquifers in the same or different valleys. It is therefore very important not only to map the valleys but also to know the age relationships between cross-cutting valleys (and other geological elements). In our study we have estimated the age relationships between different buried valleys and the glaciotectonic complex, but open questions regarding this issue still remain. The exchange of groundwater between aquifers hosted in the different geological structures

**Transboundary
geophysical mapping
of geological
elements**

F. Jørgensen et al.

[Title Page](#)[Abstract](#)[Introduction](#)[Conclusions](#)[References](#)[Tables](#)[Figures](#)[⏪](#)[⏩](#)[◀](#)[▶](#)[Back](#)[Close](#)[Full Screen / Esc](#)[Printer-friendly Version](#)[Interactive Discussion](#)

is very likely to play an important role for the entire flow regime in the area, and would probably be enhanced by the increased potential gradients due to a rising sea level.

Above, a qualitative evaluation of the impact of geological structure on saltwater migration in the study area has been formulated. A quantitative assessment of the risk of saltwater intrusion in response to sea level rise requires the use of a comprehensive density dependent flow and transport model. In addition, if reliable predictions of the exchange of saltwater between the sea, the inland aquifers and between the different formations should be carried out a detailed 3-D geological model is required. In such a model, the interpreted geological elements, as they have been described in this paper, are very critical to incorporate. A flow model would perhaps be able to give answers on some of the many open questions about the flow system and exchange between aquifers, but since the described geological elements are critical for the entire flow regime and thus for the flow calculations, it requires that these elements are properly characterised both spatially and lithologically. It is questionable, whether this task has been sufficiently fulfilled because a series of remaining basic questions still remain unanswered. These relate for instance to the extent and lithology of the lower Miocene aquifer, to the occurrence, spatial extent, and age relationships of the buried valleys, to the lack of spatial resolution of the interior of the glaciotectonic complex, and to difficulties of mapping all fault structures precisely in the entire area. On the other hand, it is evident from this study that it would not be relevant to perform a modelling exercise in this area without geophysical data. Such data must include densely collected resistivity data, which combined with borehole logs, provide an indispensable spatial overview of the geological structure and salinity distribution as well as lithological properties. In addition, seismic data may provide a detailed structural picture of the subsurface. In order to answer the open questions and thus to be able to establish and conduct unambiguous density dependent flow and transport modelling further data collection would most likely be required. Seismic data as well as borehole data and well logs, but also information on hydraulic head, salinity and groundwater age would be helpful at selected locations, especially from the deeper aquifers. Such data are important for integrated

**Transboundary
geophysical mapping
of geological
elements**

F. Jørgensen et al.

Title Page

Abstract

Introduction

Conclusions

References

Tables

Figures



Back

Close

Full Screen / Esc

Printer-friendly Version

Interactive Discussion



understanding of flow dynamics and hydrochemical evolution in groundwater systems (Gannon et al., 2012) not least when the groundwater systems are closely linked to the sea (Vandenbohede et al., 2011).

7 Conclusions

5 We have conducted a geological, physical and hydrochemical characterisation of the subsurface by a combination of airborne, surface and borehole geophysics and geological well logs in a transboundary study in the border region between Germany and Denmark. Furthermore, we have illustrated and discussed the importance of a sound understanding and description of the subsurface including the hydraulic parameters, which is of crucial importance for accurate predictions of the impacts of climate change and sea level rise in coastal regions. Detailed descriptions of geological important features such as buried valleys and fault zones and their hydraulic characteristics are of vital importance for the assessment of the impacts of climate change and sea level rise by e.g. numerical modelling.

15 *Acknowledgements.* The study is a part of the CLIWAT project, which is co-funded by The Interreg IVB North Sea Region Programme, European Union.

References

- Andersen, L. T.: The Fanø Bugt Glaciotectonic Thrust Fault Complex, Southeastern Danish North Sea. A study of large-scale glaciotectonics using highresolution seismic data and numerical modeling, Ph.D. thesis, Department of Earth Science, Aarhus University, Geological Survey of Denmark and Greenland report 2004/30, 2004.
- 20 Andersen, M. S., Baron, L., Gudbjerg, J., Gregersen, J., Chapellier, D., Jakobsen, R., and Postma, D.: Discharge of nitrate-containing groundwater into a coastal marine environment, *J. Hydrol.*, 336, 98–114, 2007.

Transboundary geophysical mapping of geological elements

F. Jørgensen et al.

Title Page

Abstract

Introduction

Conclusions

References

Tables

Figures



Back

Close

Full Screen / Esc

Printer-friendly Version

Interactive Discussion



Transboundary geophysical mapping of geological elements

F. Jørgensen et al.

Title Page

Abstract

Introduction

Conclusions

References

Tables

Figures

⏪

⏩

◀

▶

Back

Close

Full Screen / Esc

Printer-friendly Version

Interactive Discussion



- Archie, G. E.: The electrical resistivity log as an aid in determining some reservoir characteristics, *Trans. Am. Inst. Min. Metall. Pet. Eng.*, 146, 54–62, 1942.
- Auken, E. and Sørensen, K. I.: Large-scale TEM investigation for groundwater ASEG, Australia 2003, 2003.
- 5 Auken, E., Christiansen, A. V., Westergaard, J. A., Kirkegaard, C., Foged, N., and Viezzoli, A.: An integrated processing scheme for high-resolution airborne electromagnetic surveys, the SkyTEM system, *Explor. Geophys.*, 40, 184–192, 2009.
- Auken, E., Foged, N., and Sørensen, K. I.: Approaching 10 microsec (and earlier) with the SkyTEM system ASEG, 21st International Geophysical Conference and Exhibition, Sydney, 10 2010a.
- Auken, E., Kirkegaard, C., Ribeiro, J., Foged, N., and Kok, A.: The use of airborne electromagnetic for efficient mapping of salt water intrusion and outflow to the sea. SWIM21 – 21st Salt Water Intrusion Meeting, 21–26 June, Azores, Portugal, 2010b.
- Bartholdy, J. and Pejrup, M.: Holocene Evolution of the Danish Wadden Sea, *Senck. marit.*, 24, 15 187–209, 1994.
- Bear, J., Cheng, A. H. D., Sorek, S., Ouazar, D., and Herrera, I.: Seawater intrusion in coastal aquifers – concepts, methods and practices, Kluwer Academic Publishers, Dordrecht, 1999.
- Buckley, D. K., Hinsby, K., and Manzano, M.: Application of geophysical borehole logging techniques to examine coastal aquifer palaeohydrogeology, *Geol. Soc. Sp.*, 189, 251–270, 2001.
- 20 Calvache, M. L. and Pulido-Bosch, A.: Effects of geology and human activity on the dynamics of salt-water intrusion in three coastal aquifers in southern Spain, *Environ. Geol.*, 30, 215–223, 1997.
- Carrera, J., Hidalgo, J. J., Slooten, L. J., and Vázquez-Suñé, E.: Computational and conceptual issues in the calibration of seawater intrusion models, *Hydrogeol. J.*, 18, 131–145, 2010.
- 25 Cartwright, J.: The structural evolution of the Ringkøbing-Fyn High, in: *Tectonic Evolution of the North Sea Rifts*, edited by: Blundell, D. J. and Gibbs, A. D., Clarendon Press, Oxford, 200–216, 1990.
- Chang, S. W., Clement, T. P., Simpson, M. J., and Lee, K.-K.: Does sea-level rise have an impact on saltwater intrusion?, *Adv. Water Resour.*, 34, 1283–1291, 2011.
- 30 Clark, P. U. and Mix, A. C.: Ice sheets and sea level of the Last Glacial Maximum, *Quaternary Sci. Rev.*, 21, 1–7, 2002.
- Custodio, E. and Bruggeman, G. A.: *Groundwater problems in coastal areas*, UNESCO, International Hydrological Programme, Paris, 1987.

- de Louw, P. G. B., Eeman, S., Siemon, B., Voortman, B. R., Gunnink, J., van Baaren, E. S., and Oude Essink, G. H. P.: Shallow rainwater lenses in deltaic areas with saline seepage, *Hydrol. Earth Syst. Sci.*, 15, 3659–3678, doi:10.5194/hess-15-3659-2011, 2011.
- Edmunds, W. M., Hinsby, K., Marlin, C., Condesso de Melo, M. T., Manzano, M., Vaikmaa, R., and Travi, Y.: Evolution of groundwater systems at the European coastline, *Geol. Soc. Sp.*, 189, 289–311, 2001.
- Essink, G. H. P. O.: Salt water intrusion in a three-dimensional groundwater system in the Netherlands: A numerical study, *Transport Porous Med.*, 43, 137–158, 2001.
- Essink, G. H. P. O., van Baaren, E. S., and de Louw, P. G. B.: Effects of climate change on coastal groundwater systems: A modeling study in the Netherlands, *Water Resour. Res.*, 46, W00F04, doi:10.1029/2009WR008719, 2010.
- Fitterman, D. V. and Deszcz-Pan, M.: Characterization of Saltwater Intrusion in South Florida Using Electromagnetic Geophysical Methods, Proceedings of the 18th Salt Water Intrusion Meeting, 31 May–3 June 2004, Cartagena, Spain, 2004.
- Friberg, R.: Geologisk model for Tønder Nyhedsbrev, May 1989, Sønderjyllands Amt, 1989.
- Friberg, R.: The landscape below the Tinglev outwash plain. A reconstruction, *B. Geol. Soc. Denmark*, 43, 34–40, 1996
- Friberg, R. and Thomsen, S.: Kortlægning af Ribeformationen. Et fællesjysk grundvandsarbejde, Technical report, Ribe Amt, Ringkøbing Amt, Viborg Amt, Århus Amt, Vejle Amt, Sønderjyllands Amt, ISBN 87-7486-359-2, 1999.
- GEUS, the National well database (Jupiter): available at: http://geuskort.geus.dk/GeusMap/index_jupiter.jsp?imgxy=622+403&iMapWidth=1244&iMapHeight=806, last access: 15 February 2012.
- Hansen, J. M., Aagaard, T., and Binderup, M.: Absolute sea levels and isostatic changes of the eastern North Sea to central Baltic region during the last 900 years, *Boreas*, online first: doi:10.1111/j.1502-3885.2011.00229.x, 2011.
- Heck, H.-L.: Grundwasserverhältnisse und geologischer Bau im schleswig-holsteinischen Marsch- und Nordseeinselgebiet, *Sitzungsber. D. Preuss. Geol. Landesanstalt*, 6, 169–196, 1931.
- Heck, H.-L.: Das Grundwasser im Zusammenhang mit dem geologischen Bau Schleswig-Holsteins, *Preuss. Geol. Landesanstalt*, 133 pp., 1932.
- Hinsby, K., Harrar, W. G., Nyegaard, P., Konradi, P. B., Rasmussen, E. S., Bidstrup, T., Gregersen, U., and Boaretto, E.: The Ribe Formation in western Denmark; Holocene and

**Transboundary
geophysical mapping
of geological
elements**

F. Jørgensen et al.

Title Page

Abstract

Introduction

Conclusions

References

Tables

Figures

◀

▶

◀

▶

Back

Close

Full Screen / Esc

Printer-friendly Version

Interactive Discussion



- Konradi, P. B., Larsen, B., and Sørensen, A. B.: Marine Eemian in the Danish eastern North Sea, *Quatern. Int.*, 133–134, 21–31, 2005.
- Mullen, I. and Kellett, J.: Groundwater salinity mapping using airborne electromagnetics and borehole data within the lower Balonne catchment, Queensland, Australia, *Int. J. Appl. Earth Obs.*, 9, 116–123, 2007.
- Mulligan, A. E., Evans, R. L., and Lizarralde, D.: The role of paleochannels in groundwater/seawater exchange, *J. Hydrol.*, 335, 313–329, 2007.
- Nishikawa, T., Siade, A. J., Reichard, E. G., Ponti, D. J., Canales, A. G., and Johnson, T. A.: Stratigraphic controls on seawater intrusion and implications for groundwater management, Dominguez Gap area of Los Angeles, California, USA, *Hydrogeol. J.*, 17, 1699–1725, 2009.
- Nyboe, N. S., Jørgensen, F., and Sørensen, K. I.: Integrated inversion of TEM and seismic data facilitated by high penetration depths of a segmented receiver setup, *Near Surf. Geophys.*, 8, 467–473, 2010.
- Ødum, H.: Grundvandsforholdene i Tønder-Marsken, DGU, IV rk., 2, 12, 17 pp., 1934.
- Teatini, P., Tosi, L., Viezzoli, A., Baradello, L., Zecchin, M., and Silvestri, S.: Understanding the hydrogeology of the Venice Lagoon subsurface with airborne electromagnetics, *J. Hydrol.*, 411, 342–354, 2011.
- Post, V. and Abarca, E.: Preface: Saltwater and freshwater interactions in coastal aquifers RID E-6054-2011, *Hydrogeol. J.*, 18, 1–4, 2010.
- Rambøll: Seismisk kortlægning ved Tønder, unpublished report, 2010.
- Rasmussen, E. S.: Detailed mapping of marine erosional surfaces and the geometry of clinoforms on seismic data: a tool to identify the thickest reservoir sand, *Basin Res.*, 21, 721–737, 2009
- Rasmussen, E. S., Dybkjær, K., and Piasecki, S.: Lithostratigraphy of the Upper Oligocene – Miocene succession of Denmark, *Geol. Surv. Den. Greenl.*, 22, 92 pp., 2010.
- Ribeiro, J.: Interaction of salt – fresh water using airborne TEM methods, Faculty of Science – Lisbon University, 2010.
- Roth, B., Mikkelsen, P., and Auken, E.: SkyTEM Survey Tønder 2009, Leck 2008, Rens/Løgumgårde 2011, Department of Earth Sciences, Aarhus University, 2011.
- Rumpel, H.-M., Binot, F., Gabriel, G., Siemon, B., Steuer, A., and Wiederhold, H.: The benefit of geophysical data for hydrogeological 3-D modelling – an example using the Cuxhaven buried valley, *Z. Dtsch. Ges. Geowiss.*, 160, 259–269, 2009.
- Sandersen, P. B. E., Jørgensen, F., Larsen, N. K., Westergaard, J., and Auken, E.: Rapid tunnel

**Transboundary
geophysical mapping
of geological
elements**

F. Jørgensen et al.

Title Page

Abstract

Introduction

Conclusions

References

Tables

Figures

◀

▶

◀

▶

Back

Close

Full Screen / Esc

Printer-friendly Version

Interactive Discussion

Viezzoli, A., Christiansen, A. V., Auken, E., and Sørensen, K. I.: Quasi-3D modeling of airborne TEM data by Spatially Constrained Inversion, *Geophysics*, 73, F105–F113, 2008.

Viezzoli, A., Auken, E., and Munday, T.: Spatially constrained inversion for quasi 3D modelling of airborne electromagnetic data – an application for environmental assessment in the Lower Murray Region of South Australia, *Explor. Geophys.*, 40, 173–183, 2009.

Viezzoli, A., Tosi, L., Teatini, P., and Silvestri, S.: Surface water-groundwater exchange in transitional coastal environments by airborne electromagnetics: The Venice Lagoon example, *Geophys. Res. Lett.*, 37, L01402, doi:10.1029/2009GL041572, 2010.

Werner, A. D. and Simmons, C. T.: Impact of sea-level rise on sea water intrusion in coastal aquifers, *Ground Water*, 47, 197–204, 2009.

HESSD

9, 2629–2674, 2012

Transboundary geophysical mapping of geological elements

F. Jørgensen et al.

Title Page

Abstract

Introduction

Conclusions

References

Tables

Figures



Back

Close

Full Screen / Esc

Printer-friendly Version

Interactive Discussion



Transboundary geophysical mapping of geological elements

F. Jørgensen et al.

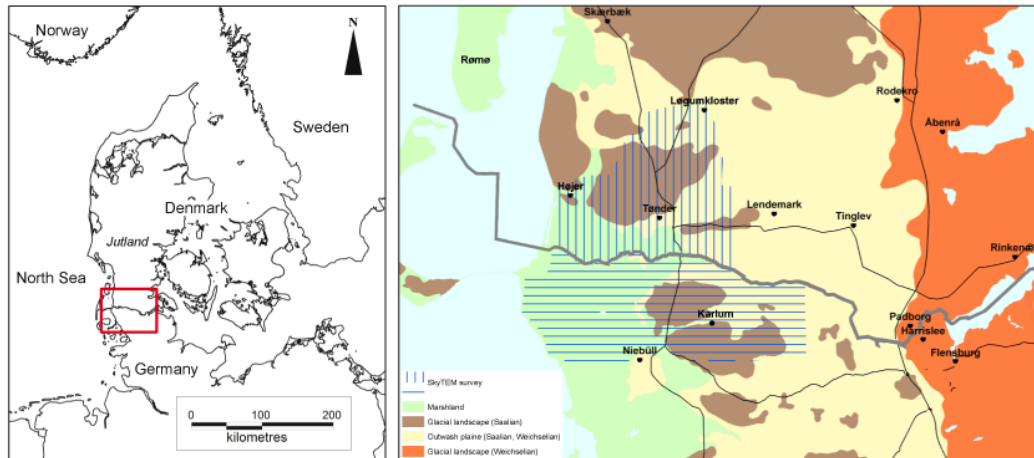


Fig. 1. Location and geography of the survey area.

Title Page

Abstract

Introduction

Conclusions

References

Tables

Figures

⏪

⏩

◀

▶

Back

Close

Full Screen / Esc

Printer-friendly Version

Interactive Discussion

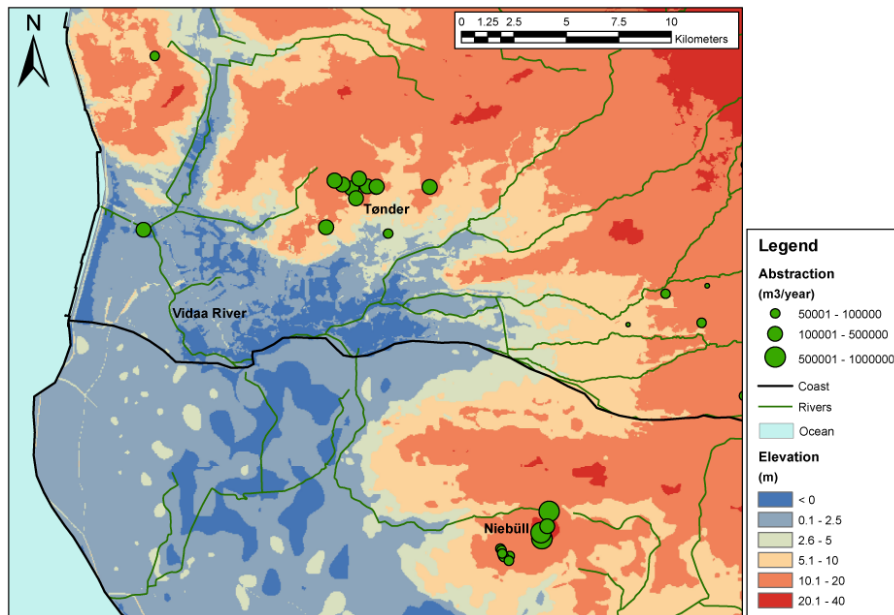


Fig. 2. Land surface elevation, drainage system and groundwater abstraction.

Transboundary geophysical mapping of geological elements

F. Jørgensen et al.

Title Page

Abstract Introduction

Conclusions References

Tables Figures

⏪ ⏩

◀ ▶

Back Close

Full Screen / Esc

Printer-friendly Version

Interactive Discussion

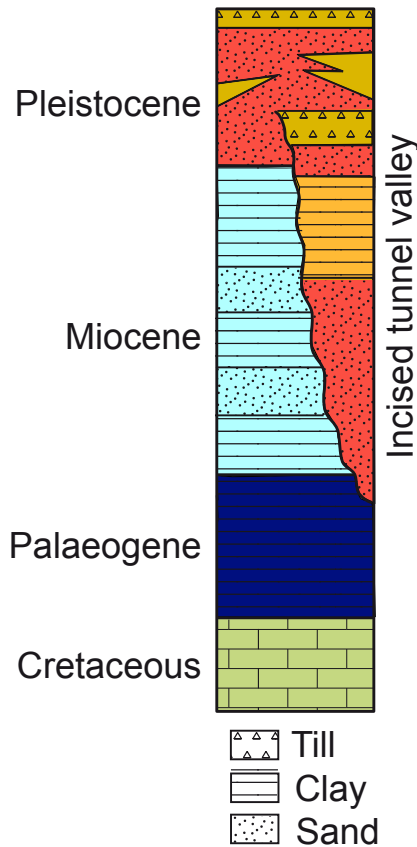


Fig. 3. Conceptual stratigraphical log for the survey area.

Transboundary geophysical mapping of geological elements

F. Jørgensen et al.

Title Page

Abstract Introduction

Conclusions References

Tables Figures

◀ ▶

◀ ▶

Back Close

Full Screen / Esc

Printer-friendly Version

Interactive Discussion

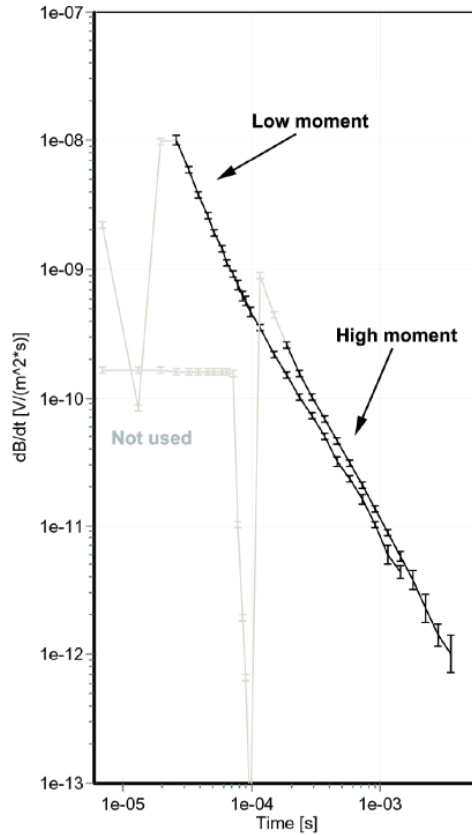
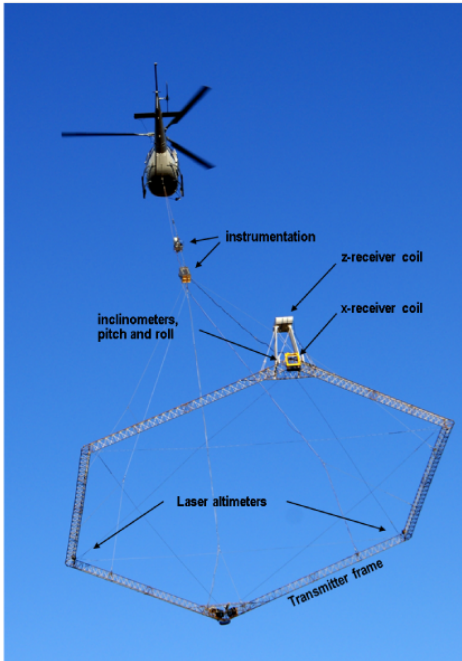


Fig. 4. Left: SkyTEM system for resistivity mapping with a Transient ElectroMagnetic (TEM) method. Right: example of a data curve divided into two moments, one giving information of the near-surface in the early times, and the other one completing the sounding model in the deeper part with measurement at the late times.

Transboundary geophysical mapping of geological elements

F. Jørgensen et al.

Title Page

Abstract

Introduction

Conclusions

References

Tables

Figures

◀

▶

◀

▶

Back

Close

Full Screen / Esc

Printer-friendly Version

Interactive Discussion

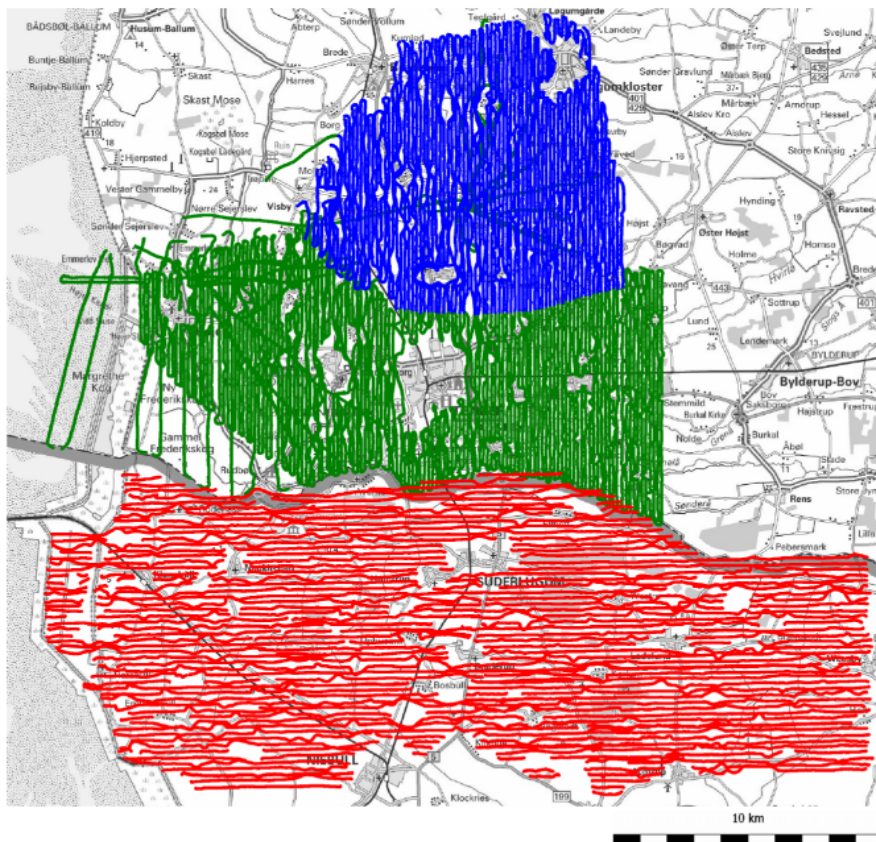


Fig. 5. The different survey areas flown by SkyTEM. The flight lines of the Tønder survey are in blue (northern part) and dark green (southern part). The flight lines of the Leck survey are in red.

**Transboundary
geophysical mapping
of geological
elements**

F. Jørgensen et al.

Title Page

Abstract

Introduction

Conclusions

References

Tables

Figures

⏪

⏩

◀

▶

Back

Close

Full Screen / Esc

Printer-friendly Version

Interactive Discussion



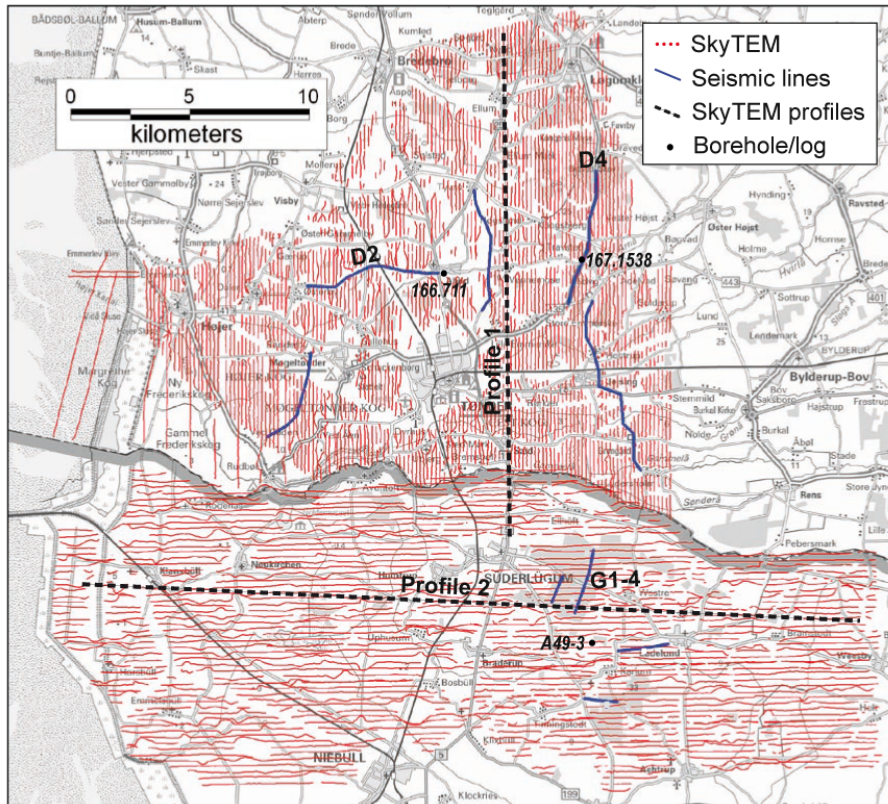


Fig. 6. Map with SkyTEM data after processing (red lines) and seismic data (blue lines). Seismic sections D2, D4 and G1–4 are shown in Fig. 7. SkyTEM profiles 1 and 2 indicated on the map are shown in Fig. 10.

HESSD

9, 2629–2674, 2012

Transboundary geophysical mapping of geological elements

F. Jørgensen et al.

Title Page

Abstract

Introduction

Conclusions

References

Tables

Figures

◀

▶

◀

▶

Back

Close

Full Screen / Esc

Printer-friendly Version

Interactive Discussion

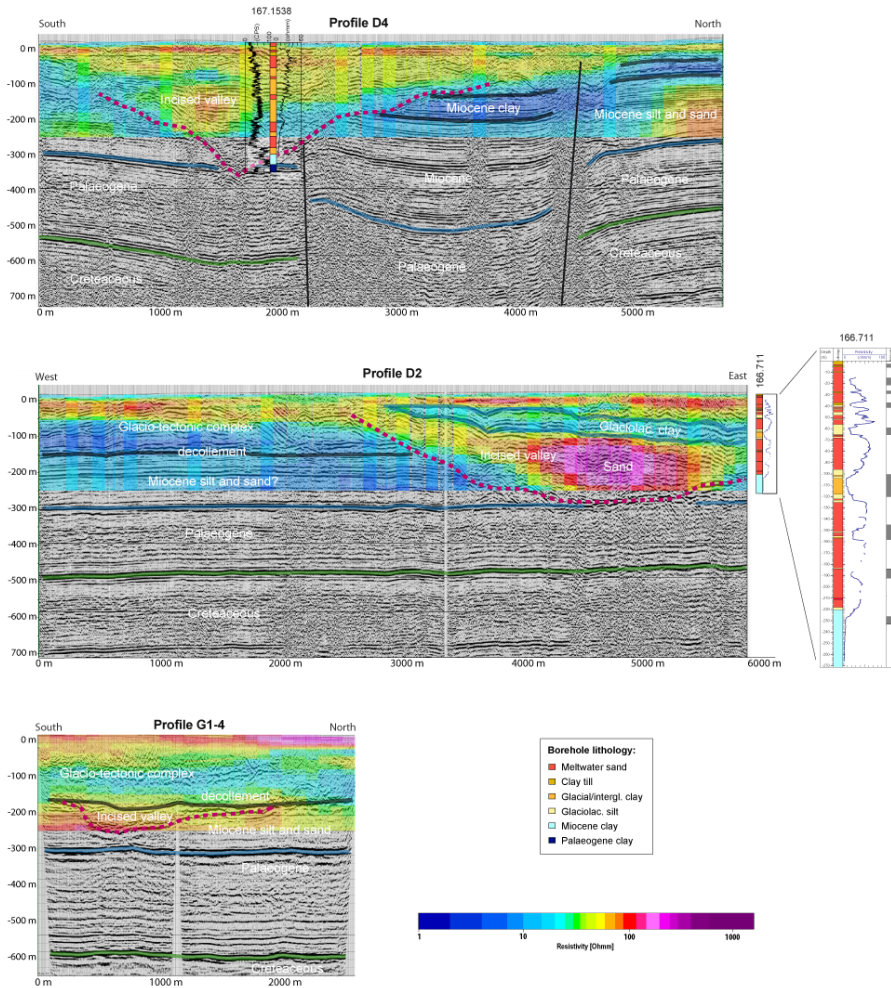


Fig. 7. Caption on next page.

Transboundary geophysical mapping of geological elements

F. Jørgensen et al.

Title Page

Abstract Introduction

Conclusions References

Tables Figures

◀ ▶

◀ ▶

Back Close

Full Screen / Esc

Printer-friendly Version

Interactive Discussion

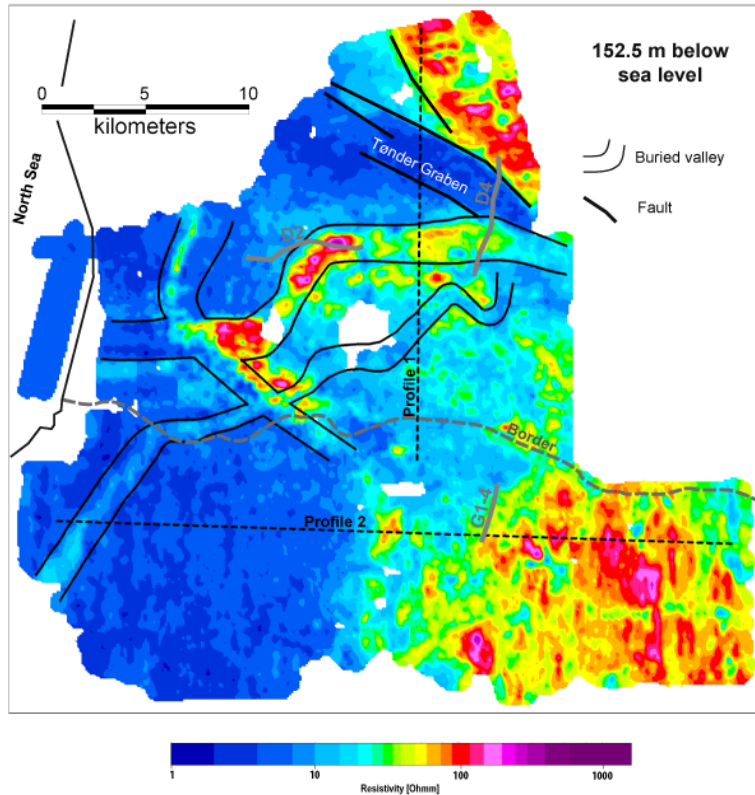


Fig. 8. Horizontal resistivity slice 152.5 m b.s.l. Faults related to the Tønder Graben are shown with thick black lines. Grey lines depict the seismic lines shown in Fig. 7. Location of the two SkyTEM profiles 1 and 2 shown in Fig. 10 are marked with dashed lines. Some of the deeper buried valleys are delineated but not necessarily expressed in the resistivity data at this specific level.

Transboundary geophysical mapping of geological elements

F. Jørgensen et al.

Discussion Paper | Discussion Paper | Discussion Paper | Discussion Paper | Discussion Paper

Title Page

Abstract Introduction

Conclusions References

Tables Figures

◀ ▶

◀ ▶

Back Close

Full Screen / Esc

Printer-friendly Version

Interactive Discussion



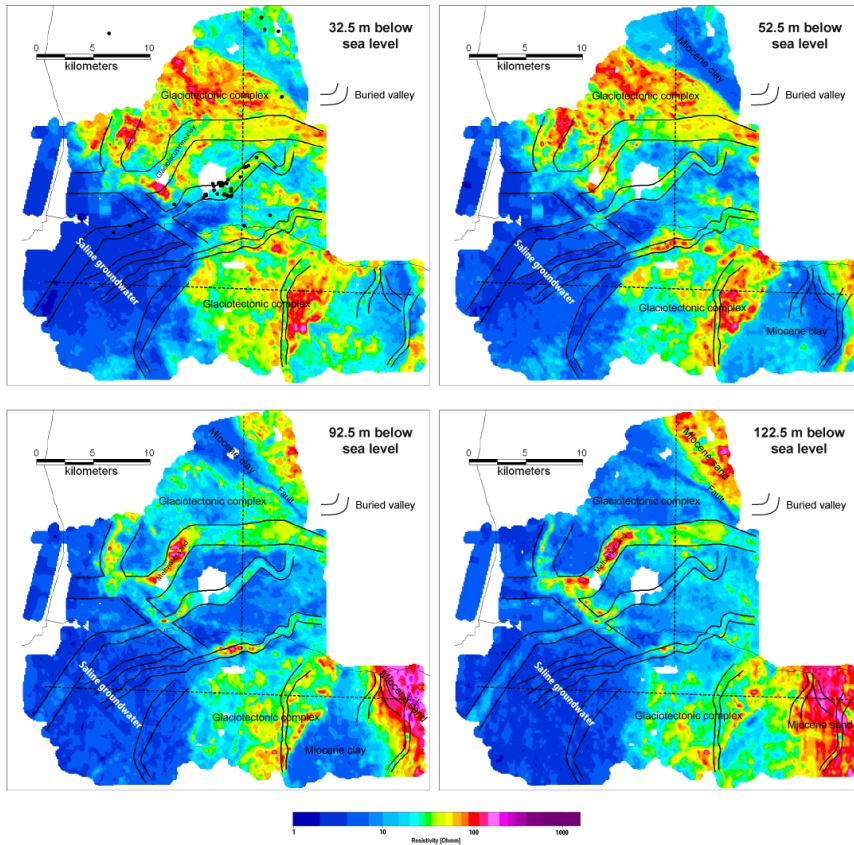


Fig. 9. Horizontal resistivity slices at four selected levels. Mapped buried valleys are outlined on the maps but not necessarily expressed in the resistivity data at each level. Boreholes with interglacial marine clay recordings are marked as black dots on 32.5 m b.s.l. This particular valley was apparently inundated by the sea during the last interglacial. Location of the two SkyTEM profiles 1 and 2 shown in Fig. 10 are marked with dashed lines.

Transboundary geophysical mapping of geological elements

F. Jørgensen et al.

Title Page

Abstract

Introduction

Conclusions

References

Tables

Figures



Back

Close

Full Screen / Esc

Printer-friendly Version

Interactive Discussion



Transboundary geophysical mapping of geological elements

F. Jørgensen et al.

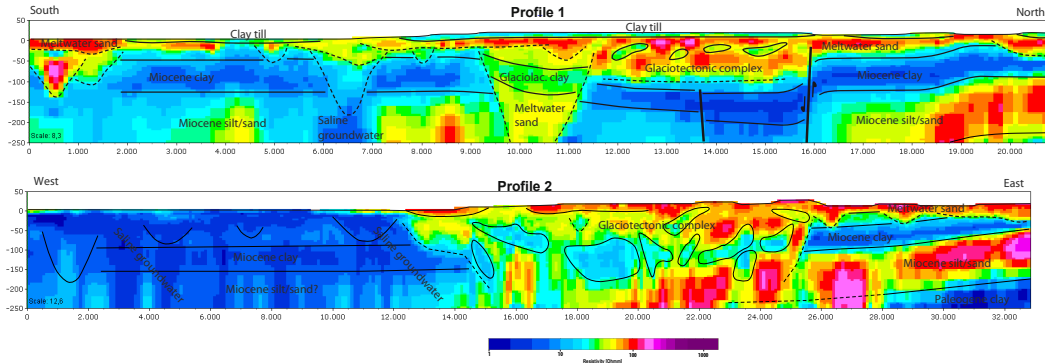


Fig. 10. Cross section profiles through the SkyTEM 3-D resistivity grid: for location see Figs. 6, 8 and 9. The deep valley seen in the seismic data on Fig. 7 is clearly seen on Profile 1 where the Miocene clay is interrupted. The Tønder Graben structure is evident in the northern part of the profile. The area is partly capped by a thin sheet of clay till. Profile 2 shows the increased salinity in the western part, the dipping Miocene clay and one of the two glaciotectonically deformed areas. Vertical exaggeration 8 and 12 x.